Research Article

Journal of Environmental Nanotechnology

Synthesis and Characterization of Fe-doped Manganese Oxide Nanoparticle by using Chemical Precipitation Method

S. Sasikala, S. Varshaa, V. Kalaiselvi*
Department of Physics, Navarasam Arts and Science College for Women, Erode, TN, India
Received: 20.10.2020 Accepted: 14.12.2020 Published: 30-12-2020
*nk.arthikalai@gmail.com

ABSTRACT

In this present study, Fe-doped Manganese Oxide nanoparticles were successfully synthesized by using the chemical precipitation method. The synthesized nanoparticles were characterized by using XRD, SEM, EDAX, FTIR, UV and PL. The average crystallite size of the sample was investigated by the XRD technique. The morphology and grain size were obtained from SEM images. The elemental composition was confirmed by EDAX. The FTIR studies confirmed the various functional groups present in the prepared sample. From the UV spectrum, the optical band gap was calculated. The intensity of emission radiation was absorbed by photoluminescence spectroscopy. This analysis confirmed that the Fe-doped MnO has a slightly greater emission band than the pure MnO.

Keywords: Chemical precipitation; Ferric Chloride; MnO; PL.

1. INTRODUCTION

Nanotechnology is a branch of science, engineering and technology, which deals with dimensions and tolerances of less than 100 nm of matter on an atomic or molecular scale. Nanoparticles have a wide application due to the unique size-dependent properties (Lu *et al.* 2012). Magnetic nanoparticles have been receiving considerable attention because of their wide range of applications, such as the immobilization of the proteins and enzymes, bio-separation, immune-assays, drug delivery and biosensors. Nanoparticles possess a high surface-to-volume ratio due to their small size, which gives very distinctive features to nanoparticles (Sagadevan *et al.* 2015). The unique chemical and physical properties of nanoparticles make them extremely suitable for designing new and improved sensing devices; especially, electrochemical sensors and biosensors (Wang *et al.* 2016). The important functions provided by nanoparticles include the immobilization of biomolecules, the catalysis of electrochemical reactions, and the enhancement of electron transfer between electrode surfaces and proteins, labeling of biomolecules and even acting as reactant (Luo *et al.* 2006)). Generally, metal oxide nanoparticles are inorganic. Various nanoparticles like Fe, Ni, Co, Mn and Zn are enormously accepted magnetic material for a wide range of applications like magnetic sensors, recording equipment, telecommunications, magnetic fluids and microwave absorbers (Zhu *et al.* 2014; Poonguzhali *et al.* 2015) . Among various metal oxide nanoparticles, manganese dioxide is an important transition metal oxide of P-type semiconducting materials (Yu *et al.* 2013). Generally, nanoparticles have been prepared by physical vapor deposition, chemical vapor deposition, aerosol processing, sol-gel process, reverse micelle method and mechanical milling (Ma *et al.* 2013; Ma *et al.* 2014). A wet chemical technique such as hydrothermal sol-gel, emulsion and conventional co-precipitation method is commercially widely used because of its cost-effective nature (Cherian *et al.* 2016). Manganese oxides are natural components of soils, aquifers and sediments, and are known to be strong adsorbents of metal ions. They are important materials with a variety of applications in different fields such as chemical sensing devices, magnetic devices, environmental pollution absorbent, catalysis, ion-sieves, rechargeable batteries, hydrogen storage media and microelectronics (Dang *et al.* 2015).

2. EXPERIMENTAL DETAILS

2.1 Chemicals and Reagents

Analytical reagent grade Manganese chloride, NaOH and Ferric chloride were used for this experiment. Double distilled water was used as a solvent throughout the experiment.

2.2 Synthesis of MnO nanoparticles

4 g of manganese chloride was taken and dissolved in 50 ml of distilled water and stirred for 30 minutes using a magnetic stirrer. Then 3 g of NaOH pellets, dissolved in 20 ml distilled water, was added to

the solution to maintain the pH level at 8. After 5 hours of stirring, the brown colour precipitate was obtained and filtered by filter paper. The collected precipitate was kept in a microwave oven at 75 W for 10 minutes. Then it was dried in a muffle furnace at 400 ºC for 4 hours. The dried nanoparticles were taken in a mortar and made into a powder.

2.3 Synthesis of Fe-doped MnO nanoparticles

4 g of manganese chloride was taken and dissolved in 50 ml distilled water and stirred for 30 minutes using a magnetic stirrer. Then 3 g of NaOH pellets, dissolved in 20 ml distilled water, was added to the solution to maintain the pH level at 8. 1 g of Ferric chloride dissolved in 10 ml of distilled water was added to the above solution. After 5 hours of stirring, the dark brown precipitate obtained was filtered by filter paper. The collected precipitate was kept in a microwave oven at 75 W for 10 minutes. Then it was dried in a muffle furnace at 400 ºC for 4 hours. The dried Fe-doped nanoparticles were taken in a mortar and made into a powder.

3. RESULTS & DISCUSSION

3.1 XRD Analysis

The XRD pattern for Fe-doped MnO nanoparticles was shown in Fig. 1. The narrow peaks in the XRD pattern indicated the crystalline nature of nanoparticles and the peaks corresponding to 2θ = 36.2°, 56.1°, 58.2° and 62.4° indicated the miller indices (101), (110), (220) and (103) respectively and represent the hexagonal shape. These results were good compared to the standard data of JCPDS Card no: 41-1442. The crystallite size of the Fe-doped MnO nanoparticles was found to be 11.5 nm. The crystallite size of the particles was calculated by using the Debye-Scherrer formula,

$$D = k\lambda / \beta \cos\theta$$

where, D - Crystallite size, λ - Wavelength of the X-Ray source (1.5406 Å), β - Full width at half-maximum of the diffraction peak, k – Scherrer's constant with value 0.9 to 1 and θ - Bragg's angle.

Table 1. XRD result of Fe-doped MnO nanoparticles.

Sample	2θ	FWHM	Crystallite Size (nm)	Average Size (nm)
Fe-doped MnO	36.2	0.78980	10.4938	11.5706
	56.1	0.52070	16.8742	
	58.2	0.77110	11.4855	
	62.4	1.21250	7.42887	

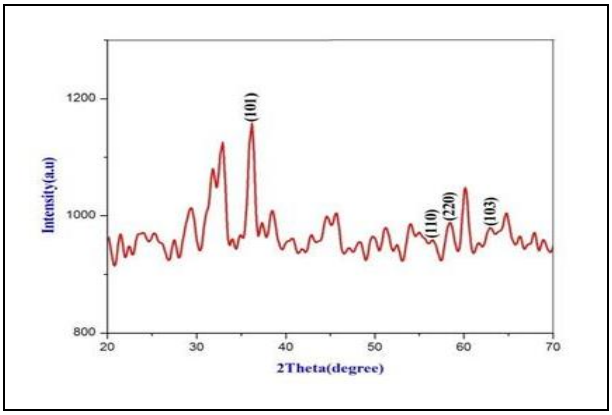

Fig. 1: XRD pattern for Fe-doped MnO nanoparticles.

3.2 SEM Analysis

Scanning Electron Microscope (SEM) was used to deduce the particle size and morphology of the synthesized Fe-doped manganese oxide nanoparticles. Fig. 2 shows that the particles were having nearly sphere-like structures. They clearly show randomly distributed grains with smaller size. The size of the synthesized Fe-doped manganese oxide nanoparticles was found to be in the range of 40-71.44 nm.

3.3 EDAX Analysis

EDAX analysis is used to indicate the elemental composition present in the sample. Manganese (Mn), Oxide (O) and Iron (Fe) peaks (Fig. 3) indicated the presence of Fe-doped MnO nanoparticles.

3.4 FT-IR Analysis

Fourier Transform Infrared Spectroscopy (FTIR) was used to identify the chemical bonds in a molecule by producing an infrared absorption spectrum. It was used to analyze the functional groups and other impurities present in the Fe-doped Manganese Oxide nanoparticles as shown in Fig. 4. FT-IR spectra of Fe-doped Manganese Oxide were recorded in the range of 400-4000 cm^{-1}. The absorption spectrum in the excitation of bond gives the various stretching of functional groups.

3.5 UV Visible Spectroscopy Analysis

The optical property and bandgap energy of the samples were determined from UV absorbance. The UV Visible spectra of Fe-doped MnO nanoparticles were shown in Fig. 5. The spectra were recorded in the range of 200-900 nm. The maximum absorbance peak was at 223 nm. The bandgap energy (E_g) value of the Fe-doped MnO nanoparticle was 5.57 eV. The bandgap energy was calculated by,

$$Eg = h\upsilon = hc / \lambda$$

where, h - Planck's constant (6.626×10^{-34} m^2 kg/s), λ - wavelength (nm), υ - frequency and c – the speed of light (3×10^8 m/s).

3.6 Photo Luminescence Analysis

The intensity of emission radiations was observed by Photoluminescence spectroscopy. The emission radiation of Fe-doped MnO nanoparticles was shown in Fig. 3.6. The excitation wavelength occurs at the range of 269.8 nm for pure and Fe-doped MnO nanoparticles. The emission band of pure and Fe-doped MnO nanoparticles were located at 295 nm and 296 nm.

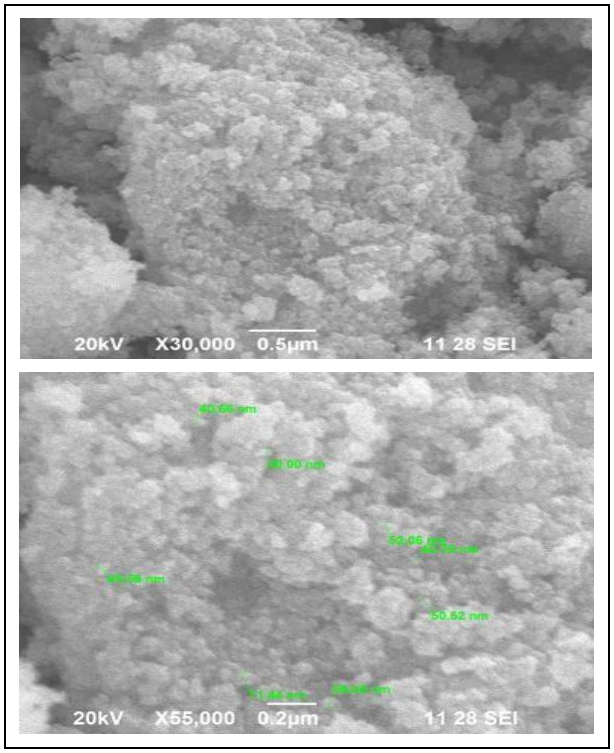

Fig. 2: SEM images of Fe-doped MnO nanoparticles.

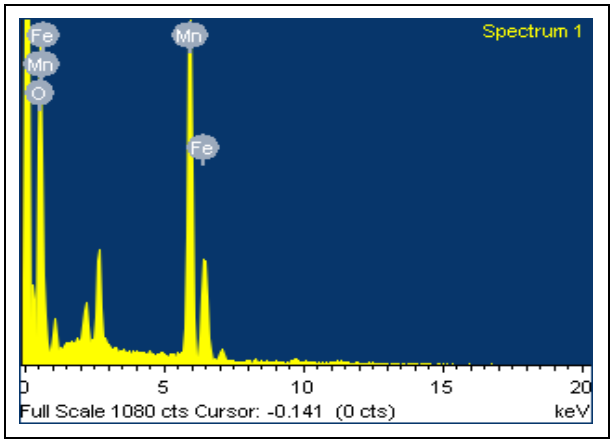

Fig. 3: EDAX analysis for Fe-doped MnO nanoparticles.

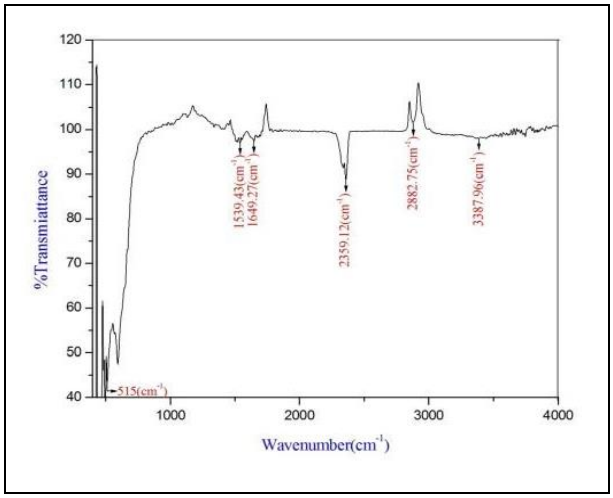

Fig. 4: FTIR spectrum of Fe-doped MnO nanoparticles.

Table 2: FTIR peaks of Fe-doped MnO nanoparticles.

Band Range (cm^{-1})	Stretching	Intensity
1539.43	N=O	Strong
1649.27	C=O	Strong
2359.12	NH+	Strong
2882.75	Symmetric CH	Very Strong
3387.96	O-H	Strong
515	Mn-O	Strong

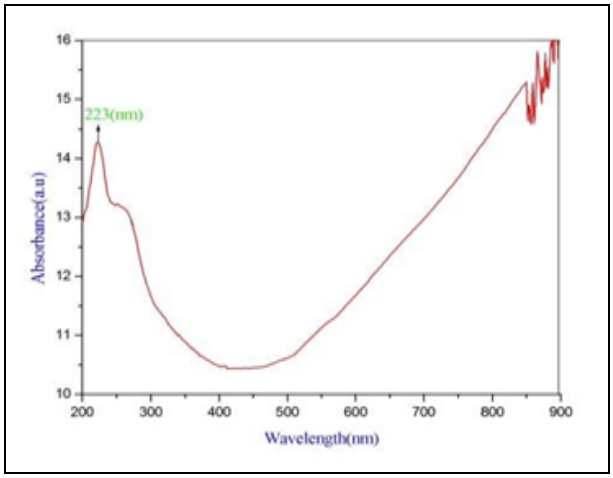

Fig. 5: Absorption spectra of Fe-doped MnO nanoparticles.

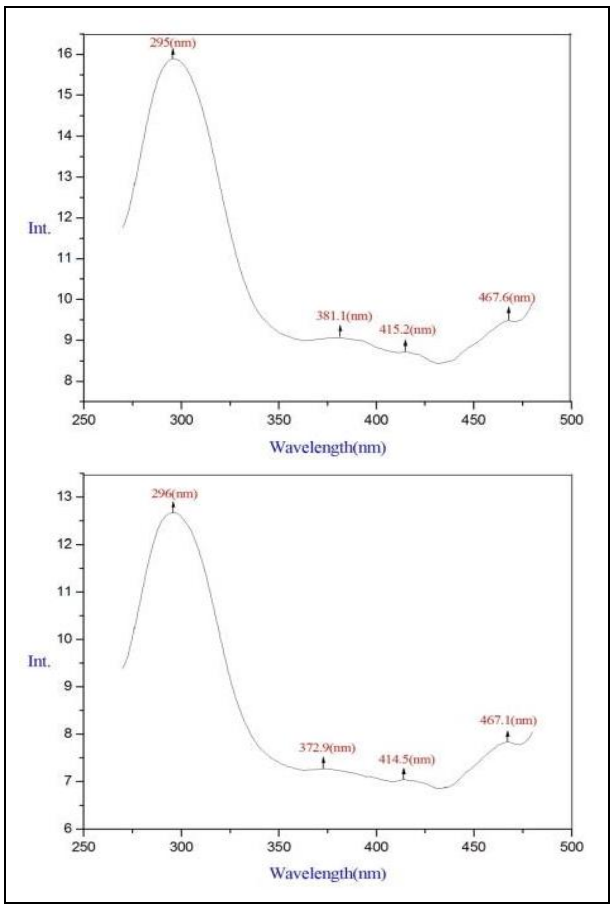

Fig. 6: Photoluminescence Analyses of Pure and Fe-doped MnO nanoparticles.

4. CONCLUSION

In this present study, the pure and Fe-doped MnO nanoparticles were synthesized by using the chemical precipitation method and then characterized by using XRD, SEM, EDAX, FTIR, UV and PL. The crystallite size of Fe-doped MnO nanoparticles prepared by chemical precipitation method was 11.5 nm, and it had a hexagonal shape. SEM images showed a nearly sphere-shaped morphological structure. The presence of elemental composition was confirmed by EDAX. The FTIR studies confirmed the various functional groups present in the prepared sample. In UV analysis, the bandgap energy for Fe-doped MnO nanoparticle was at the range of 5.57 nm. The emission band of pure and Fe-doped MnO nanoparticles were located at 295 nm and 296 nm, as analyzed by PL. The Fe-doped MnO nanoparticle had a slightly greater emission band than the pure MnO nanoparticle.

FUNDING

This research received no specific grant from any funding agency in the public, commercial, or not-for-profit sectors.

CONFLICTS OF INTEREST

The authors declare that there is no conflict of interest.

COPYRIGHT

REFERENCES

Cherian, E., Rajan, A. and Baskar, G., Synthesis of manganese dioxide nanoparticles using co-precipitation method and its antimicrobial activity, *Int. J. Mod. Sci. Technol.*, 01, 17–22 (2016).

Dang, T. D., Le, T. T. H., Hoang, T. B. T. and Mai, T. T., Synthesis of nanostructured manganese oxides based materials and application for supercapacitor, *Adv. Nat. Sci. Nanosci. Nanotechnol.*, 6(2), 025011 (2015). https://dx.doi.org/10.1088/2043-6262/6/2/025011

Lu, X., Yu, M., Wang, G., Zhai, T., Xie, S., Ling, Y., Tong, Y. and Li, Y., H-TiO_2 @MnO_2//H-TiO_2 @C core-shell nanowires for high performance and flexible asymmetric supercapacitors, *Adv. Mater.*, 25(2), 267–272 (2013). https://dx.doi.org/10.1002/adma.201203410

Luo, X., Morrin, A., Killard, A. J. and Smyth, M. R., Application of nanoparticles in electrochemical sensors and biosensors, *Electroanalysis*, 18(4), 319–326 (2006). https://dx.doi.org/10.1002/elan.200503415

Ma, Y., Fang, C., Ding, B., Ji, G. and Lee, J. Y., Fe-doped Mn_xO_y with hierarchical porosity as a high-performance lithium-ion battery anode, *Adv. Mater.*, 25(33), 4646–4652 (2013). https://dx.doi.org/10.1002/adma.201301906

Ma, Z., Huang, X., Dou, S., Wu, J., Wang, S., One-Pot synthesis of Fe_2O_3 nanoparticles on nitrogen-doped graphene as advanced supercapacitor electrode materials, *J. Phys. Chem. C.*, 118(31), 17231–17239 (2014). https://dx.doi.org/10.1021/jp502226j

Poonguzhali, R., Shanmugam, N., Gobi, R., Senthilkumar, A., Viruthagiri, G. and Kannadasan, N., Effect of Fe doping on the electrochemical capacitor behavior of MnO_2 nanocrystals, *J. Power Sources.*, 293, 790–798 (2015). https://dx.doi.org/10.1016/j.jpowsour.2015.06.021

Sagadevan, S., Investigations on synthesis, structural, morphological and dielectric properties of manganese oxides nanoparticles, *J. Material. Sci. Eng.*, 4(3), 1000172(2015). https://dx.doi.org/10.4172/2169-0022.1000172

Wang, Z., Wang, F., Li, Y., Hu, J., Lu, Y. and Xu, M., Interlinked multiphase Fe-doped MnO_2 nanostructures: A novel design for enhanced pseudocapacitive performance, *Nanoscale*, 8(13), 7309-7317 (2016). https://dx.doi.org/10.1039/c5nr08857g

Yu, Z., Duong, B., Abbitt, D. and Thomas, J., Highly ordered MnO_2 nanopillars for enhanced supercapacitor performance, *Adv. Mater.*, 25(24), 3302-3306 (2013). https://dx.doi.org/10.1002/adma.201300572

Zhu, J., Tang, S., Xie, H., Dai, Y. and Meng, X., Hierarchically porous MnO_2 microspheres doped with homogeneously distributed Fe_3O_4 nanoparticles for supercapacitors, *ACS Appl. Mater. Interfaces*, 6(20), 17637-17646 (2014). https://dx.doi.org/10.1021/am505622c